

Structural and vibrational studies on composites polymer electrolytes $(\text{PEO})_{10}\text{CF}_3\text{COONa} + x \text{ wt.}\% \text{Al}_2\text{O}_3$

Estudios estructurales y vibracionales en compósitos $(\text{PEO})_{10}\text{CF}_3\text{COONa} + x \text{ wt.}\% \text{Al}_2\text{O}_3$
 Nori Magali Jurado-Meneses¹, Miguel Iban Delgado-Rosero^{1*}, Miguel Angel Meléndez-Lira²

¹Grupo de Investigación de Materiales Semiconductores y Superiónicos, Departamento de Física, Facultad de Ciencias, Universidad del Tolima. Calle 42 Carrera 3 Barrio Altos de Santa Helena. A. A. 546. Ibagué, Colombia.

²Departamento de Física, Centro de Investigaciones y de Estudios Avanzados del Instituto Politécnico Nacional (CINVESTAV). Av. Instituto Politécnico Nacional 2508, Col. San Pedro Zacatenco. C. P. 07360. Ciudad de México, México.

ARTICLE INFO

Received August 09, 2016

Accepted March 23, 2017

KEYWORDS

Composites, Raman spectroscopy, infrared spectroscopy, ionic conductivity

Compositos, espectroscopía Raman, espectroscopía infrarroja, conductividad iónica

ABSTRACT: Composites formed by combinations of polyethylene oxide (PEO) and sodium trifluoroacetate (CF_3COONa) with different aluminum oxide (Al_2O_3) concentrations were synthesized. Infrared (IR), Raman spectroscopy, X ray diffraction (XRD) and atomic force microscopy (AFM) analyses, were performed to characterize the composites. Changes on the XRD intensity peaks, and variations in intensity and position of some peaks in Raman and IR spectroscopy were observed for different concentrations of added Al_2O_3 . The decrease in the XRD peaks of the PEO when it is combined with the salt, revealed that crystallinity in polymer was reduced, being lower when the alumina is added. The increase in roughness root medium square (R_{RMS}) observed by AFM when Al_2O_3 was added, agree with reduction in crystallinity observed with XRD studies. Changes in the structure of PEO showed in the absorption lines IR and Raman, due to addition of CF_3COONa salt and Al_2O_3 filler, have been attributed to the interactions between the electrolyte and the filler.

RESUMEN: Se sintetizaron compósitos formados entre polióxido de etileno (PEO) y trifluoroacetato de sodio ($\text{PEO}_{10}\text{CF}_3\text{COONa}$) con diferentes concentraciones de óxido de aluminio (Al_2O_3). Los compósitos fueron caracterizados por espectroscopía infrarroja (IR), espectroscopía Raman, difracción de rayos X (XRD) y microscopía de fuerza atómica (AFM). Las combinaciones del electrolito sólido $\text{PEO}_{10}\text{CF}_3\text{COONa}$ con diferentes concentraciones de Al_2O_3 , mostraron cambios en la intensidad de los picos de XRD, así como cambios en la intensidad y posición de algunos picos de IR y Raman. El decrecimiento de los picos del PEO en XRD, cuando este fue combinado con la sal, reveló que la cristalinidad del polímero se redujo, siendo más baja cuando se le adicionó alúmina. Se observó un incremento en la raíz cuadrática media de la rugosidad (R_{RMS}) obtenida por microscopía de fuerza atómica cuando se adicionó Al_2O_3 . Este incremento está en concordancia con la reducción de la cristalinidad observada con estudios de XRD. Los cambios en la estructura del PEO mostrados en las líneas de absorción de IR y Raman, debidos a la adición de CF_3COONa y Al_2O_3 , fueron atribuidos a interacciones entre el electrolito y el relleno Al_2O_3 .

1. Introduction

Due to the growing need for production and storage of energy in a safe and environmentally friendly way, in the recent decades many researchers have focused on the development of solid polymer electrolytes (SPE) as essential component in various electrochemical devices. The SPE are polymers with insulating properties mixed with

substances that provide ions such as salts and acids. These ions, which are coordinate with polymer atoms, provide the ionic conduction required for applications in rechargeable batteries, electrochromic windows, fuel cells and humidity sensors, and in wide variety of portable devices [1]. The diversity of shapes and sizes, and the operating conditions of these devices, have generated great interest in the search of SPE with properties such as higher ionic conductivity ($\sigma > 1 \times 10^{-5} \text{ S cm}^{-1}$), better mechanical flexibility and wider thermal and electrochemical windows. In this context, previous studies of composites obtained by combinations of solid electrolytes with fillers as Al_2O_3 , SiO_2 and TiO_2 have reported an enhancement in the ionic mobility due to increases in the amorphous phase, without loss of mechanics, thermal and electrochemical properties [2].

* Corresponding author: Miguel Iban Delgado Rosero

e-mail: mirosero@ut.edu.co

ISSN 0120-6230

e-ISSN 2422-2844

Up to date, the fillers play an important role in the properties of composites. For example, in polymer electrolytes formed with polyethylene oxide (PEO), the fillers affect the polymer dipoles orientation in their ability to align dipole moments [3], whereas the thermal history determines the flexibility of the polymer chains for ion migration [2]. Usually, the addition of fillers in SPE like PEO with alkaline salts, improves the transport properties, the resistance to crystallization, and the stability of the electrode/electrolyte interface [2, 4].

In general, the increase in conductivity of solid electrolytes at room temperature has been the main goal of investigations in this field. In this regard, some of the most relevant changes in conductivity of polymer electrolytes added with fillers have been explained in literature by: (i) the interactions of filler grains with ions creating pathways of high conductivity in the vicinity of grains, and weaken the association between ion pairs and enhance the transference number [5–10]; (ii) the higher fraction of amorphous phase in the polymer host at room temperature; (iii) the size and chemical composition of filler able to penetrate into the polymer matrix and interact with components of composite [11, 12]; (iv) the filler-filler interactions that allow the formation of percolation network for ions, which avoid the crystallization of polymer increasing the amorphous phase between filler grains [13]; (v) the availability of charge carriers and the coordination sites on the polymer electrolyte [14, 15].

In order to get a better understanding of what causes the observed changes in composites conductivity, various techniques of characterization have been used. The IR and Raman spectroscopy have been widely used for polymer electrolytes and composites characterization [2, 16, 17], because they allow identifying and quantifying of specific intra and inter polymer chain molecular interactions. Spectroscopy studies on the PEO-LiCF₃SO₃ system, showed a series IR bands assigned to ion CF₃SO₃⁻, which change when its environment is modified by the presence of polymer [18]. Ion-polymer, ion-ion, polymer-filler and polymer-ion-filler interactions are studied by Raman and X ray diffraction (XRD); variations of width, intensity and shift of the bands with the formation of other peaks of specific bonds give information regarding some of these interactions [19].

The changes of conductivity previously reported in systems such as PEO/CF₃COOLi [20] and PEO/CF₃COONa [21], have motivated us to the study of the composite formed by PEO/CF₃COONa added with Al₂O₃ as filler, with the goal of increasing the conductivity in this system and knowing more about the interaction polymer-salt, polymer-filler and electrolyte-filler. In this paper, we studied the (PEO)₁₀CF₃COONa + *x* wt.% Al₂O₃ system by XRD, Raman, and IR to obtain information about changes in crystallinity due to interactions between the components of system. Additionally, we analyzed membranes morphology by AFM and obtained roughness root square medium (R_{RSM}).

2. Experimentation

PEO (molecular weight M_w = 1x10⁶) and CF₃COONa were purchased from Aldrich and dried under vacuum conditions (~500 Pa). The reactants were stored in dry atmosphere with silica gel and then weighed in a 10:1 ratio (EO:Na) before being dissolved separately in acetonitrile while magnetically stirred for four hours. Both solutions were combined and stirred for other four hours. Subsequently, Al₂O₃ (~ 150 mesh and 50 Å of size pore) was added at percentages of 0.0, 3.0, 10.0, 20.0, 30.0 with relation to the whole electrolyte (i.e, $x = \text{wt. Al}_2\text{O}_3 / (\text{wt. Al}_2\text{O}_3 + \text{wt. (PEO)}_{10}\text{CF}_3\text{COONa}) * 100 \%$). The mixtures were constantly stirred magnetically to prevent Al₂O₃ particles decantation and to ensure the uniform dispersion in the electrolyte. The mixtures were casted in a glass Petri dish where the solvent evaporated slowly at room temperature inside a desiccator under dry conditions. The resulting membranes had mechanical consistency with thickness between 150 ± 10 µm and 200 ± 10 µm.

The samples of (PEO)₁₀CF₃COONa + *x* wt.% Al₂O₃ were analyzed by XRD on a Siemens D5000 system employing the Cu Kα wavelength with a grazing incidence angle of 3°. The IR spectra were obtained with a Nicolet 750 Fourier transform infrared system. Raman spectroscopy was carried out on a Horiba Jobin Yvon LabRAM system, employing the 632.8 nm of one HeNe laser as an excitation source. The morphology was analyzed with atomic force microscopy (Autoprobe CP Research), and the Roughness Root Square Medium (R_{RSM}) was obtained with the WSxM software [22].

3. Results and discussion

3.1 X ray diffraction

Figure 1 shows the XRD patterns for pure PEO, solid electrolyte (PEO)₁₀CF₃COONa (*x* = 0.0%) and (PEO)₁₀CF₃COONa + *x* wt.% Al₂O₃ for different *x* values (*x* = 3.0; 10.0; 20.0; 30.0). The XRD pattern of pure PEO membrane shows the characteristic peaks for this polymer at 2θ = 19.3° and 23.6° [7, 23].

In the polymer electrolyte PEO₁₀CF₃COONa diffractogram (*x* = 0.0% in Figure 1), new peaks at 19.4°, 24.1° and 25.0°, compared to PEO diffractogram, are observed. These peaks correspond to the crystalline nature of new complex (PEO)₁₀CF₃COONa formed by the coordination of alkaline ions like Na⁺ with oxygen atoms of PEO. The decrease in the crystallinity of pure PEO, is evidenced in the decrease of the intensity of the peaks at 19.3° and 23.6° [8]. The results obtained for PEO₁₀CF₃COONa are consistent with DSC results reported by J. Castillo *et al.* [21].

On the other hand, diffractograms of the composites (PEO)₁₀CF₃COONa + *x* wt.% Al₂O₃ show a remarkable reduction of the XRD peaks intensity as the Al₂O₃ concentration increases. The reduction of the peaks intensity is attributed to the reorganization in the PSE

structure and to an increase in the amorphous phase by adding Al_2O_3 . The increase of amorphous nature give more flexibility to the backbone, resulting in a composite with greater ionic diffusivity and a higher ionic conductivity than the $\text{PEO}_{10}\text{CF}_3\text{COONa}$, as previously was reported by N. M Jurado *et al.* [24].

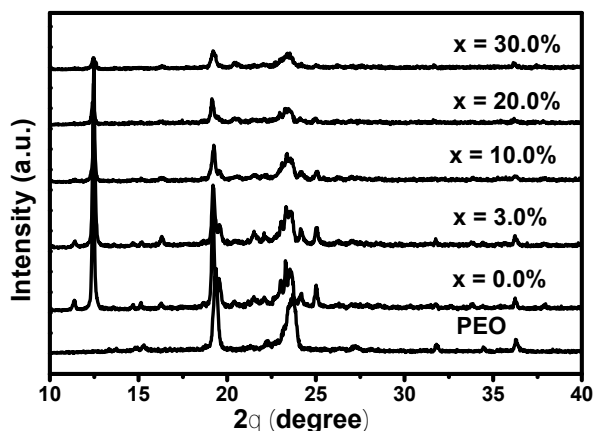


Figure 1 X ray diffractograms membranes of pure PEO and $(\text{PEO})_{10}\text{CF}_3\text{COONa} + x \text{ wt.}\% \text{Al}_2\text{O}_3$ ($x = 0.0$; 3.0; 10.0; 20.0; 30.0)

3.2 Raman spectroscopy

Figure 2 shows the Raman spectra of the PEO pure, the salt CF_3COONa and the $(\text{PEO})_{10}\text{CF}_3\text{COONa} + x \text{ wt.}\% \text{Al}_2\text{O}_3$ composites studied. The broad peak present at 235 cm^{-1} (a in Figure 2) has been assigned to the disordered longitudinal acoustic mode (D-LAM) of PEO [25]. The same peak is observed, without significant changes, in the spectrum of PEO pure and $(\text{PEO})_{10}\text{CF}_3\text{COONa}$, and on all composites added with Al_2O_3 .

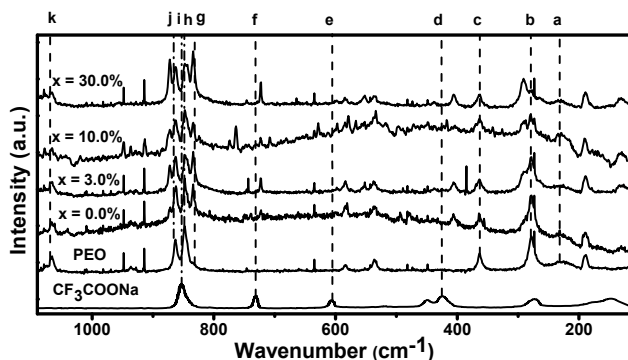


Figure 2 Raman spectra of CF_3COONa , PEO, $(\text{PEO})_{10}\text{CF}_3\text{COONa}$ and different Al_2O_3 concentrations in the electrolyte

The peak shown at 279 cm^{-1} in the Raman spectrum of PEO (b in Figure 2), has been assigned to O-C-C/C-O-C bending and C-C rocking [25]. The broadening and weakening of this

peak as a function of Al_2O_3 concentration, indicates that the PEO polymer chain tends to adopt different conformations due to the interaction between the ether groups and the hydrogen bonds [16, 25]. Similarly, mild changes are observed on intensity and width in spectral line assigned to C-O-C/O-C-C bending vibrations of pure PEO at 364 cm^{-1} , (c in the Figure 2). These variations are due to the changes in the PEO structure by formation of complex with alkaline-metals salts as Li^+ and Na^+ [25].

The peak observed at 424 cm^{-1} in CF_3COONa spectrum (d in the Figure 2), corresponding to C-C-O-O out of plane bending [26], has been displaced to 404 cm^{-1} in the solid electrolyte $(\text{PEO})_{10}\text{CF}_3\text{COONa}$, and its combinations with Al_2O_3 likely due to the presence of crystalline PEO. This shift in the Raman band by the presence of small crystallites of a different material, has been observed in the combination of polymers such as PEO and PVDF-HFP [27].

The weak spectral line corresponding to CF_3 symmetric bending in CF_3COONa at 606 cm^{-1} [26, 28] (e in the Figure 2), is not present in spectra of electrolyte $(\text{PEO})_{10}\text{CF}_3\text{COONa}$ or the composites $(\text{PEO})_{10}\text{CF}_3\text{COONa} + x \text{ wt.}\% \text{Al}_2\text{O}_3$, this indicate that the salt was dissolved in polymer. Additionally, the spectral line corresponding to CF_3 deformation umbrella in the salt [29, 30] (at 731 cm^{-1} , f in the Figure 2), is displaced to 722 cm^{-1} when it is combined with the PEO, and all composites added with the filler. These changes in CF_3 are attributed to ionic-association in ion-pairs by coordination of anions and cations [31, 32].

The weak shoulder around 830 cm^{-1} in the spectrum of pure PEO, which has been previously reported [33] (g in Figure 2), is clearly resolved when the PEO is combined with the CF_3COONa and the different filler concentrations. The peaks observed in pure PEO at 848 and 862 cm^{-1} (h and j in Figure 2), are attributed to the CH_2 rocking and C-O stretching vibrational modes respectively [25]. However, a new peak close to these lines (at 872 cm^{-1}) appears in the Raman spectrum when the salt is added, and increases its intensity with the addition of Al_2O_3 . This new spectral line confirms the change in the structure of the PEO chain by interactions ion-polymer. On that subject, it has been frequently observed that systems formed by PEO combined with alkaline salts show dramatic changes in frequency and intensities between 770 and 900 cm^{-1} ; these changes are associated to the change in the backbone of the PEO [34]. Further, the increase of the intensity of the new peaks likely is due to interaction filler-polymer that deforms the structure by the presence of filler. In this region, the spectral line that corresponds to C-C stretching of salt appears at 853 cm^{-1} (i in the Figure 2), which is combined with the spectral lines of PEO indicated interactions from the ion-polymer.

The line corresponding to the combination of C-O-C symmetric stretching and CH_2 symmetric rocking at $1,066 \text{ cm}^{-1}$ of PEO [35] (k in the Figure 2) is also present in the electrolyte $(\text{PEO})_{10}\text{CF}_3\text{COONa}$ and the composites with slight changes in intensity and width, due to variations in the conformational structure of polymer.

The appearance of new lines in the Raman spectra when the polymer was combined with salt, confirm the formation of complex; these results agree with the formation of new peaks in the XRD diffractograms of the combination of PEO and CF_3COONa . The semi-crystalline character of samples are affected by addition of Al_2O_3 particles, that addition increase the amorphous phase in the new composite, producing changes in the intensity and broadening of the Raman peaks.

3.3. Infrared spectroscopy

Figure 3 shows the IR spectra for pure PEO, CF_3COONa , the polymer electrolyte $(\text{PEO})_{10}\text{CF}_3\text{COONa}$ and $(\text{PEO})_{10}\text{CF}_3\text{COONa} + x \text{ wt.}\% \text{ Al}_2\text{O}_3$ composites, between 1,000 and 450 cm^{-1} . For the electrolyte $\text{PEO}_{10}\text{CF}_3\text{COONa}$ with low concentrations of Al_2O_3 , the line assigned to CF_3 asymmetric bending of in CF_3COONa at 534 cm^{-1} [29, 36, 37] (a in Figure 3) overlaps the lines at 508 and 529 cm^{-1} assigned to C-O-C stretching of in the principal chain of PEO [38, 39]; however, for the highest Al_2O_3 concentration the three peaks are clearly defined.

The line assigned to CF_3 symmetric bending at 741 cm^{-1} in the spectrum of CF_3COONa [40] (b in Figure 3), has shifted to 718 cm^{-1} , when was combined with PEO and Al_2O_3 . Similarly, the C-C stretching mode at 820 cm^{-1} [36, 40] in CF_3COONa (c in Figure 3) shifted to 803 cm^{-1} when it was combined with PEO. The line assigned to CH_2 wagging in the PEO is observed at 842 cm^{-1} (d in Figure 3) [18]. At higher concentrations of Al_2O_3 ($x \geq 10\%$), multiples lines appear between 797-872 cm^{-1} . The broad band assigned to CH_2 twisting at 991 cm^{-1} in PEO (e in Figure 3) [18], split into multiples lines at high concentrations of Al_2O_3 . The formation of new lines in the range of 797-892 cm^{-1} and 992-995 are likely due to the effect of polymer-filler and ion-polymer interactions.

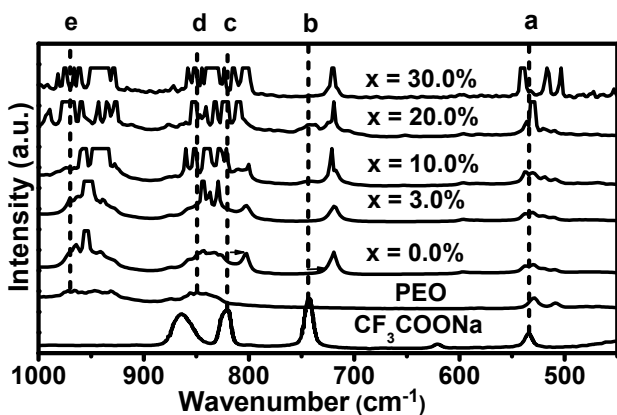


Figure 3 IR spectra of CF_3COONa , PEO and electrolyte $(\text{PEO})_{10}\text{CF}_3\text{COONa}$ with different Al_2O_3 concentrations in $(\text{PEO})_{10}\text{CF}_3\text{COONa}$, between 1,000 and 450 cm^{-1}

The IR spectra for range 1,000-1,500 cm^{-1} is shown in Figure 4. For pure PEO, the lines corresponding to the C-O-C stretching mode at 1,061 cm^{-1} , 1,107 cm^{-1} and 1,149 cm^{-1} , are present [41] (a, b, c in the Figure 4); when PEO is combined with salt and Al_2O_3 multiples lines appearance. For CF_3COONa , two broad peaks are attributed to CF_3 asymmetric and symmetric stretching at 1,167 cm^{-1} and 1,223 cm^{-1} respectively [26, 29] (d and e in Figure 4).

The broad band present between 1,326 cm^{-1} and 1,360 cm^{-1} (f in the Figure 4), corresponding to CH_2 asymmetric wagging PEO [42] split into two clear lines when it is combined with the CF_3COONa and into four lines when the filler is added. The line corresponding to C-O-O symmetric stretching of CF_3COONa observed at 1,394 cm^{-1} [29] (g in the Figure 4) is not present either in the spectrum of solid electrolyte $(\text{PEO})_{10}\text{CF}_3\text{COONa}$ or in any of the composites this indicate that salt was dissolved in the polymer. The peak present at 1,412 cm^{-1} in the spectrum of pure PEO (h in the Figure 4) is displaced to 1,426 cm^{-1} when it is combined with the salt and increases the broadness when Al_2O_3 is added. The broad band presented in the spectrum of pure PEO between 1,448 cm^{-1} and 1,476 cm^{-1} (i in the Figure 4) is assigned to the combination of CH_2 asymmetric bending and CH_2 scissoring modes [42, 43]. Finally, the band corresponding to C-O-O symmetric stretching mode of CF_3COONa [29] (j in the Figure 4) is observed to 1,477 cm^{-1} . All these broad bands split into multiples peaks for higher concentrations of filler ($x \geq 10\%$).

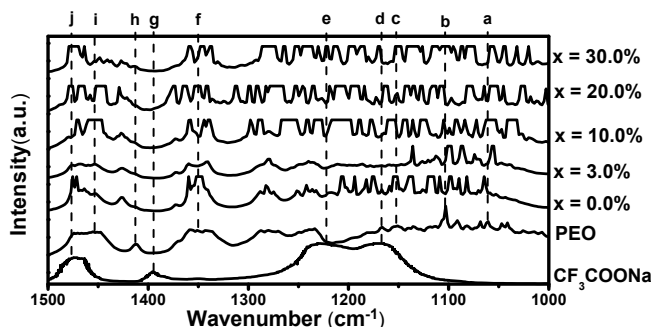


Figure 4 IR spectra for PEO, CF_3COONa , $(\text{PEO})_{10}\text{CF}_3\text{COONa}$ and composites $(\text{PEO})_{10}\text{CF}_3\text{COONa} + x \text{ wt.}\% \text{ Al}_2\text{O}_3$, between 1,000 cm^{-1} and 1,500 cm^{-1}

The shift of IR bands of CF_3COONa when it is combined with PEO is attributed to changes in the environment of CF_3COO^- ions that interact with the polymer chain. In addition, the shift of IR peaks of PEO when it is combined with salt is attributed to coordination of oxygen atoms in polymer chain with Na^+ ions of the salt. When the Al_2O_3 is added, the broadness of the peaks increased; it means that the amorphous phase increased, creating conduction pathways in the surface of Al_2O_3 particles and avoiding crystallization of $(\text{PEO})_{10}\text{CF}_3\text{COONa}$ complex. All these contribute to enhance the ionic mobility in the amorphous phase increasing the conductivity [24].

3.4. Atomic force microscopy

Figure 5 shows three-dimensional AFM images in the range of the scan areas $5\ \mu\text{m} \times 5\ \mu\text{m}$ for the membrane surfaces of solid electrolyte $(\text{PEO})_{10}\text{CF}_3\text{COONa}$ (Figure 5(a)), $(\text{PEO})_{10}\text{CF}_3\text{COONa} + 3\ \text{wt.}\% \text{Al}_2\text{O}_3$ (Figure 5(b)), $(\text{PEO})_{10}\text{CF}_3\text{COONa} + 20\ \text{wt.}\% \text{Al}_2\text{O}_3$ (Figure 5(c)) and $(\text{PEO})_{10}\text{CF}_3\text{COONa} + 30\ \text{wt.}\% \text{Al}_2\text{O}_3$ (Figure 5(d)) composites. The changes observed in the membranes surface morphology are correlated with the Roughness Root Medium Square (R_{RMS}) and the Roughness Average (R_a), and were computed by WSxM software [22] and reported in Table 1. The increases in the R_{RMS} with the addition of the filler indicates a decrease in crystallinity [44], probably due to the fact that Al_2O_3 particles are surround by amorphous material.

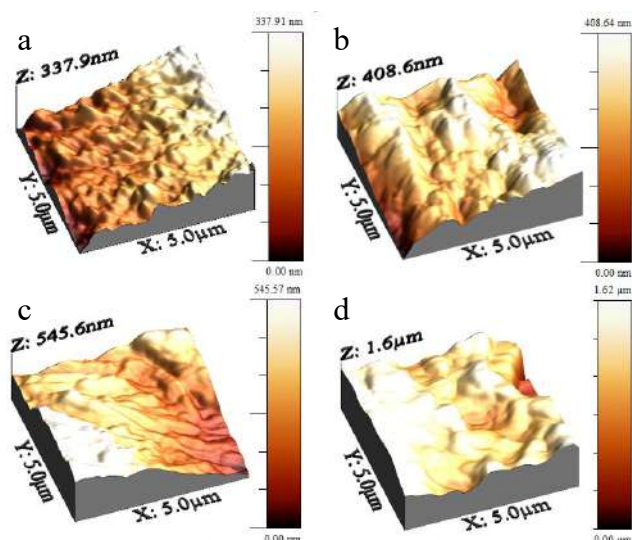


Figure 5 AFM micrographs of: a) electrolyte $(\text{PEO})_{10}\text{CF}_3\text{COONa}$; b) composite $(\text{PEO})_{10}\text{CF}_3\text{COONa} + 3\ \text{wt.}\% \text{Al}_2\text{O}_3$; c) composite $(\text{PEO})_{10}\text{CF}_3\text{COONa} + 20\ \text{wt.}\% \text{Al}_2\text{O}_3$; d) composite $(\text{PEO})_{10}\text{CF}_3\text{COONa} + 30\ \text{wt.}\% \text{Al}_2\text{O}_3$

Table 1 Roughness Root Square Medium (R_{RSM}) for membranes of PEO, $(\text{PEO})_{10}\text{CF}_3\text{COONa}$ and composites $(\text{PEO})_{10}\text{CF}_3\text{COONa} + x\ \text{wt.}\% \text{Al}_2\text{O}_3$ in areas of $5\ \mu\text{m} \times 5\ \mu\text{m}$

Membrane	R_{RMS} (nm)	R_a (nm)
$(\text{PEO})_{10}\text{CF}_3\text{COONa}$	63.77	52.66
$x = 3.0\%$	67.30	52.55
$x = 20.0\%$	115.0	95.25
$x = 30.0\%$	221.4	167.2

4. Conclusions

The appearance of new peaks, variation in intensity, and shifting of the peaks in the XRD, IR, and Raman spectra

for $(\text{PEO})_{10}\text{CF}_3\text{COONa}$ membrane with respective to salt and polymer, confirm the formation of a new complex. The change in the conformational structure of PEO is due to the coordination of polymer with Na^+ cations. The changes observed in the salt spectrum by modification of ionic environment, due to interactions of CF_3COO^- anion with polymer. These results agree with previous studies of impedance spectroscopy and differential scanning calorimetric, where a new endothermic anomaly corresponding to melting crystalline phase, and an enhancement of conductivity are observed in relation of pure PEO [45].

The fraction of crystalline phase in the volume of the new $(\text{PEO})_{10}\text{CF}_3\text{COONa}$ electrolyte is also affected by the addition of Al_2O_3 particles. The increase in amorphous phase fraction of composites $(\text{PEO})_{10}\text{CF}_3\text{COONa} + x\ \text{wt.}\% \text{Al}_2\text{O}_3$ improve the conductivity values, by migration of ions Na^+ through the pathways of amorphous phase surrounding the filler. This has been previously reported by N.M. Jurado *et al.* [24]. The disruption of crystallization of the SPE host matrix, by effect of Al_2O_3 addition, is evidenced by changes in the intensity and broadness of IR and Raman bands, and by loss of the intensity in RXD diffractograms peaks. In some composites, the increase in the ionic conductivity is proportional to the amorphicity [46], however, for the $(\text{PEO})_{10}\text{CF}_3\text{COONa} + x\ \text{wt.}\% \text{Al}_2\text{O}_3$ system, Al_2O_3 concentrations greater than 3% results in a loss of ionic conductivity due to the blocking effect of filler particles, which hinders the motions of mobile ions.

Similarly, the loss of crystallinity in membranes is validated by the morphology changes observed in the AFM micrographs; further the increases in roughness as a function of Al_2O_3 concentration point to an increase in the amorphous phase of the membrane [47].

5. Acknowledgements

This work was supported by the Central Research Committee of the University of Tolima (project 430113). The authors are grateful to laboratory of characterization at CINVESTAV-México D.F for AFM measures and for technical support by R. Frago.

6. References

1. H. S. Han, C. Cho, S. Y. Kim, and J. M. Hyun, "Performance evaluation of a polymer electrolyte membrane fuel cell system for powering portable freezer," *Appl. Energy*, vol. 105, pp. 125-137, 2013.
2. M. R. Johan, O. H. Shy, S. Ibrahim, S. M. Mohd, and T. Y. Hui, "Effects of Al_2O_3 nanofiller and EC plasticizer on the ionic conductivity enhancement of solid $\text{PEO-LiCF}_3\text{SO}_3$ solid polymer electrolyte," *Solid State Ionics*, vol. 196, no. 1, pp. 41-47, 2011.
3. B. Kumar, S. J. Rodrigues, and R. J. Spry, "Dipoles and their possible effects on conductivity in polymer-ceramic composite electrolytes," *Electrochim. Acta*, vol. 47, no. 8, pp. 1275-1281, 2002.

4. H. J. Walls *et al.*, "Fumed silica-based composite polymer electrolytes: Synthesis, rheology, and electrochemistry," *J. Power Sources*, vol. 89, no. 2, pp. 156–162, 2000.
5. F. Croce, G. B. Appetecchi, L. Persi, and B. Scrosati, "Nanocomposite polymer electrolytes for lithium batteries," *Nature*, vol. 394, pp. 456–458, 1998.
6. F. Croce *et al.*, "Role of the ceramic fillers in enhancing the transport properties of composite polymer electrolytes," *Electrochim. Acta*, vol. 46, no. 16, pp. 2457–2461, 2001.
7. M. Marcinek *et al.*, "Effect of filler surface group on ionic interactions in PEG-LiClO₄-Al₂O₃ composite polyether electrolytes," *J. Phys. Chem. B*, vol. 104, no. 47, pp. 11088–11093, 2000.
8. W. Wieczorek, Z. Florjanczyk, and J. R. Stevens, "Composite polyether based solid electrolytes," *Electrochim. Acta*, vol. 40, no. 13-14, pp. 2251–2258, 1995.
9. T. J. Singh and S. V. Bhat, "Increased lithium-ion conductivity in (PEG)₄₀-LiClO₄ solid polymer electrolyte with δ-Al₂O₃ nanoparticles," *J. Power Sources*, vol. 129, no. 2, pp. 280–287, 2004.
10. Z. Wang, Y. Hu, and L. Chen, "Some studies on electrolytes for lithium ion batteries," *J. Power Sources*, vol. 146, no. 1-2, pp. 51–57, 2005.
11. T. Mohamed, N. Padmanathan, and S. Selladurai, "Effect of nanofiller CeO₂ on structural, conductivity, and dielectric behaviors of plasticized blend nanocomposite polymer electrolyte," *Ionics*, vol. 21, no. 3, pp. 829–840, 2015.
12. L. Tadiello *et al.*, "The filler-rubber interface in styrene butadiene nanocomposites with anisotropic silica particles: morphology and dynamic properties," *Soft Matter*, vol. 11, no. 20, pp. 4022–4033, 2015.
13. M. Mariano, N. El Kissi, and A. Dufresne, "Cellulose nanocrystals and related nanocomposites: Review of some properties and challenges," *J. Polym. Sci. Part B: Polym. Phys.*, vol. 52, no. 12, pp. 791–806, 2014.
14. J. Zhou and P. S. Fedkiw, "Ionic conductivity of composite electrolytes based on oligo(ethylene oxide) and fumed oxides," *Solid State Ionics*, vol. 166, no. 3-4, pp. 275–293, 2004.
15. K. Vignarooban, M. Dissanayake, I. Albinsson, and B. Mellander, "Ionic conductivity enhancement in PEO:CuSCN solid polymer electrolyte by the incorporation of nickel-chloride," *Solid State Ionics*, vol. 278, pp. 177–180, 2015.
16. A. Pereira *et al.*, "Effect of starch type on miscibility in poly(ethylene oxide) (PEO)/starch blends and cytotoxicity assays," *Mater. Sci. Eng.: C.*, vol. 31, no. 2, pp. 443–451, 2011.
17. Y. Kumar, S. A. Hashmi, and G. P. Pandey, "Lithium ion transport and ion-polymer interaction in PEO based polymer electrolyte plasticized with ionic liquid," *Solid State Ionics*, vol. 201, no. 1, pp. 73–80, 2011.
18. S. Ramesh, T. F. Yuen, and C. J. Shen, "Conductivity and FTIR studies on PEO-LiX [X: CF₃SO₃⁻, SO₄²⁻] polymer electrolytes," *Spectrochim. Acta - Part A: Mol. Biomol. Spectrosc.*, vol. 69, no. 2, pp. 670–675, 2008.
19. N. Shukla and A. K. Thakur, "Enhancement in electrical and stability properties of amorphous polymer based nanocomposite electrolyte," *J. Non. Cryst. Solids*, vol. 357, no. 22-23, pp. 3689–3701, 2011.
20. R. Meziane, J. P. Bonnet, M. Courty, K. Djellab, and M. Armand, "Single-ion polymer electrolytes based on a delocalized polyanion for lithium batteries," *Electrochim. Acta*, vol. 57, pp. 14–19, 2011.
21. J. Castillo, I. Delgado, M. Chacón, and R. A. Vargas, "New solid ionic conductor based on poly(ethylene oxide) and sodium trifluoroacetate," *Electrochim. Acta*, vol. 46, no. 10-11, pp. 1695–1697, 2001.
22. I. Horcas *et al.*, "WSXM: a software for scanning probe microscopy and a tool for nanotechnology," *Rev. Sci. Instrum.*, vol. 78, no. 1, pp. 013705-1–013705-8, 2007.
23. S. Klongkan and J. Pumchusak, "Effects of Nano Alumina and Plasticizers on Morphology, Ionic Conductivity, Thermal and Mechanical Properties of PEO-LiCF₃SO₃ Solid Polymer Electrolyte," *Electrochim. Acta*, vol. 161, pp. 171–176, 2015.
24. N. M. Jurado, I. Delgado, and R. A. Vargas, "Conductividad iónica en nuevos compósitos (PEO)₁₀ (CF₃COONa)-X % Al₂O₃," *Univ. Sci.* vol. 18, no. 2, pp. 173–180, 2013.
25. S. K. Chaurasia, R. K. Singh, and S. Chandra, "Ion-polymer complexation and ion-pair formation in a polymer electrolyte PEO:LiPF₆ containing an ionic liquid having same anion: A Raman study," *Vib. Spectrosc.*, vol. 68, pp. 190–195, 2013.
26. G. A. Crowder, "Infrared spectra of trifluoroacetate esters," *Journal of Fluorine Chemistry*, vol. 1, no. 2, pp. 219–225, 1971.
27. S. Das and A. Ghosh, "Structure, ion transport, and relaxation dynamics of polyethylene oxide/poly(vinylidene fluoride co-hexafluoropropylene) - Lithium bis(trifluoromethane sulfonyl) imide blend polymer electrolyte embedded with ionic liquid," *J. Appl. Phys.*, vol. 119, no. 9, pp. 095101-1–095101-9, 2016.
28. T. K. Gounev, G. A. Guirgis, and J. R. Durig, "Vibrational spectra, conformational stability and ab initio calculations of trifluoromethylsulfonyl isocyanate," *J. Mol. Struct.*, vol. 436-437, pp. 613–625, 1997.
29. K. O. Christe, "Vibrational spectra of trifluoroacetates," *Spectrochim. Acta Part A: Mol. Spectrosc.*, vol. 29, no. 12, pp. 2017–2024, 1973.
30. H. Beckers, H. Bürger, and R. Eujen, "Vibrational spectra and normal coordinate analysis of CF₃ compounds: Part XLVII. Vibrational spectra, normal coordinate analysis and electron diffraction investigation of CF₃SiH₃ and its deuterated varieties," *Journal of Molecular Structure*, vol. 140, no. 3-4, pp. 281–301, 1986.
31. L. J. Hardwick, M. Holzappel, A. Wokaun, and P. Novák, "Raman study of lithium coordination in EMI-TFSI additive systems as lithium-ion battery ionic liquid electrolytes," *J. Raman Spectrosc.*, vol. 38, no. 1, pp. 110–112, 2007.
32. C. Sequeira and D. Santos, *Polymer electrolytes: fundamentals and applications*, 1st ed. Cambridge, UK: Woodhead Publishing, 2010.
33. B. Mattsson *et al.*, "Raman scattering investigations of PEO and PPO sulphonic acids," *Solid State Ionics*, vol. 97, no. 1-4, pp. 309–314, 1997.

34. C. M. Burba, "Local Structures in PEO-[C₂mim]CF₃SO₃ Electrolytes Used in Electrochemical Double-Layer Capacitors," *ECS Trans.*, vol. 13, no. 17, pp. 3-11, 2008.
35. J. Maxfield and I. W. Shepherd, "Conformation of poly(ethylene oxide) in the solid state, melt and solution measured by Raman scattering," *Polymer*, vol. 16, no. 7, pp. 505-509, 1975.
36. R. E. Robinson and R. C. Taylor, "Raman spectrum and vibrational assignments for the trifluoroacetate ion," *Spectrochim. Acta*, vol. 18, no. 8, pp. 1093-1097, 1962.
37. C. P. Rhodes and R. Frech, "A symmetry-based analysis of Raman and infrared spectra of the compounds [poly(ethylene oxide)]₃LiCF₃SO₃ and [poly(ethylene oxide)]NaCF₃SO₃," *Solid State Ionics*, vol. 136-137, pp. 1131-1137, 2000.
38. S. Yang, Z. Liu, Y. Liu, and Y. Jiao, "Effect of molecular weight on conformational changes of PEO: an infrared spectroscopic analysis," *J. Mater. Sci.*, vol. 50, no. 4, pp. 1544-1552, 2015.
39. C. Bergeron, E. Perrier, A. Potier, and G. Delmas, "A Study of the Deformation, Network, and Aging of Polyethylene Oxide Films by Infrared Spectroscopy and Calorimetric Measurements," *Int. J. Spectrosc.*, vol. 2012, pp. 1-13, 2012.
40. G. A. Crowder and D. Jackson, "Infrared and Raman spectra of methyl trifluoroacetate," *Spectrochim. Acta Part A: Mol. Spectrosc.*, vol. 27, no. 9, pp. 1873-1877, 1971.
41. A. R. Polu, D. K. Kim, and H. W. Rhee, "Poly(ethylene oxide)-lithium difluoro(oxalato)borate new solid polymer electrolytes: ion-polymer interaction, structural, thermal, and ionic conductivity studies," *Ionics*, vol. 21, no. 10, pp. 2771-2780, 2015.
42. Z. Shen, G. P. Simon, and Y. B. Cheng, "Comparison of solution intercalation and melt intercalation of polymer-clay nanocomposites," *Polymer*, vol. 43, no. 15, pp. 4251-4260, 2002.
43. K. N. Kumar, M. Kang, K. Sivaiah, M. Ravi, and Y. C. Ratnakaram, "Enhanced electrical properties of polyethylene oxide (PEO) + polyvinylpyrrolidone (PVP):Li⁺ blended polymer electrolyte films with addition of Ag nanofiller," *Ionics*, vol. 22, no. 6, pp. 815-825, 2016.
44. S. Jayanthi, A. Arulsankar, and B. Sundaresan, "NanoSrTiO₃-filled PEO-P(VdF-HFP)-LiClO₄ electrolytes with improved electrical and thermal properties," *Appl. Phys. A*, vol. 122: 109, 2016.
45. I. Delgado, J. Castillo, M. Chacón, and R. A. Vargas, "Ionic Conductivity in the Polymer Electrolytes PEO/CF₃COONa," *Physica status solidi (b)*, vol. 220, no. 1, pp. 625-629, 2000.
46. B. Scrosati, F. Croce, and L. Persi, "Impedance Spectroscopy Study of PEO-Based Nanocomposite Polymer Electrolytes," *J. Electrochem. Soc.*, vol. 147, no. 5, pp. 1718-1721, 2000.
47. P. Prabakaran and R. P. Manimuthu, "Enhancement of the electrochemical properties with the effect of alkali metal systems on PEO/PVdF-HFP complex polymer electrolytes," *Ionics*, vol. 22, no. 6, pp. 827-839, 2016.